Intravenously delivered multilineage-differentiating stress enduring cells dampen excessive glutamate metabolism and microglial activation in experimental perinatal hypoxic ischemic encephalopathy

Toshihiko Suzuki[1,2] , Yoshiaki Sato[1], Yoshihiro Kushida[3],
Masahiro Tsuji[4] , Shohei Wakao[3], Kazuto Ueda[1,2], Kenji Imai[5],
Yukako Iitani[5], Shinobu Shimizu[6] , Hideki Hida[7] ,
Takashi Temma[8], Shigeyoshi Saito[8], Hidehiro Iida[8],
Masaaki Mizuno[6], Yoshiyuki Takahashi[2], Mari Dezawa[3],
Cesar V Borlongan[9] and Masahiro Hayakawa[1]

Abstract

Perinatal hypoxic ischemic encephalopathy (HIE) results in serious neurological dysfunction and mortality. Clinical trials of multilineage-differentiating stress enduring cells (Muse cells) have commenced in stroke using intravenous delivery of donor-derived Muse cells. Here, we investigated the therapeutic effects of human Muse cells in an HIE model. Seven-day-old rats underwent ligation of the left carotid artery then were exposed to 8% oxygen for 60 min, and 72 hours later intravenously transplanted with 1×10^4 of human-Muse and -non-Muse cells, collected from bone marrow-mesenchymal stem cells as stage-specific embryonic antigen-3 (SSEA-3)+ and −, respectively, or saline (vehicle) without immunosuppression. Human-specific probe revealed Muse cells distributed mainly to the injured brain at 2 and 4 weeks, and expressed neuronal and glial markers until 6 months. In contrast, non-Muse cells lodged in the lung at 2 weeks, but undetectable by 4 weeks. Magnetic resonance spectroscopy and positron emission tomography demonstrated that Muse cells dampened excitotoxic brain glutamatergic metabolites and suppressed microglial activation. Muse cell-treated group exhibited significant improvements in motor and cognitive functions at 4 weeks and 5 months. Intravenously transplanted Muse cells afforded functional benefits in experimental HIE possibly via regulation of glutamate metabolism and reduction of microglial activation.

[1]Division of Neonatology, Center for Maternal-Neonatal Care, Nagoya University Hospital, Nagoya, Japan
[2]Department of Pediatrics, Nagoya University Graduate School of Medicine, Nagoya, Japan
[3]Department of Stem Cell Biology and Histology, Tohoku University Graduate School of Medicine, Sendai, Japan
[4]Department of Regenerative Medicine and Tissue Engineering, National Cerebral and Cardiovascular Center, Osaka, Japan
[5]Department of Obstetrics and Gynaecology, Nagoya University Graduate School of Medicine, Nagoya, Japan
[6]Department of Advanced Medicine, Nagoya University Hospital, Nagoya, Japan
[7]Department of Neurophysiology and Brain Sciences, Nagoya City University Graduate School of Medical Sciences, Nagoya, Japan

[8]Department of Bio-Medical Imaging, National Cerebral and Cardiovascular Center, Osaka, Japan
[9]Department of Neurosurgery and Brain Repair, University of South Florida Morsani College of Medicine, Tampa, FL, USA

Corresponding authors:

Yoshiaki Sato, Division of Neonatology, Center for Maternal-Neonatal Care, Nagoya University Hospital, 65 Tsurumai-cho Showa-ku, Nagoya 466-8550, Japan.
Email: yoshiaki@med.nagoya-u.ac.jp

Cesar V Borlongan, Department of Neurosurgery and Brain Repair, University of South Florida College of Medicine, 12901 Bruce B. Downs Blvd., Tampa, FL 33612, USA.
Email: cborlong@usf.edu

Introduction

Perinatal hypoxic ischemic encephalopathy (HIE) manifests as an ischemic brain injury caused by asphyxia in or around birth[1] and leads to cerebral palsy, intellectual disability, and even neonatal death in some severe cases.[2] Currently, hypothermia serves as the sole effective therapy for perinatal HIE, but with effects limited, particularly in complicated cases.[3,4] Therefore, the development of novel treatments for perinatal HIE stands as an urgent clinical need.

In recent years, cell therapy using several types of stem cells[5], such as neural stem cells[6,7] and umbilical cord blood cells,[8,9] has emerged as an experimental treatment for HIE. Mesenchymal stem cells (MSCs) pose as a potential source for transplantable cells as evidenced by their therapeutic effects in rat and mouse HIE models.[10] The postulated mechanism of MSCs implicates trophic effects delivered by cytokines and nutritional factors,[11,12] but the transplanted cells display only transient engraftment into the host tissue, thereby preventing long-term therapeutic effects.[13]

Multilineage-differentiating stress enduring cells (Muse cells), harvested from bone marrow (BM), blood and organ connective tissues, display endogenous pluripotent-like property and express pluripotent surface marker stage-specific embryonic antigen-3 (SSEA-3).[14,15] Muse cells exhibit several unique transplantable cell features including non-tumorigenicity, stress tolerance, self-renewal.[16] They express sphingosine-1-phosphate (S1P) receptor 2 and can accumulate to damaged site by sensing S1P, produced by damaged cells, enabling them to selectively home to damaged site.[17,18] Following engraftment, Muse cells spontaneously differentiate into multiple tissue-constituent cells to replenish damaged cells and repair the tissue.[17–21] Therefore, Muse cells do not require induction or genetical manipulation for exhibiting pluripotency or to differentiate into target cell type for clinical use. Intravenous drip represents a minimally invasive method of administration, thus allowing Muse cell delivery in acute clinical setting. In addition, since Muse cells possess an immunomodulatory system similar to the placenta, represented by the expression of human leukocyte antigen (HLA)-G, and express interferon gamma-induced indoleamine-2,3 dioxygenase, a mediator of immunosuppression,[19] intravenously injected allogenic Muse cells were shown to survive as functional cells over 6 months in the host tissue without immunosuppressant.[17] Based on these attractive translational properties, clinical trials for stroke, acute myocardial infarction, epidermolysis bullosa and spinal cord injury have been initiated via Japanese regulatory authority, all based on intravenous drip of donor-derived allogeneic Muse cells without

HLA matching and immunosuppressant treatment (Japan Pharmaceutical Information Center-Clinical Trials Information; JapicCTI-183834, 184103, 184563, and 194841). Because of some overlapping pathology between adult stroke and perinatal HIE, the present study examined the potential therapeutic effects of Muse cells in an animal model of HIE.

Materials and methods

An expanded version of the Materials and Methods is available in the online Data Supplement. All animal experiments received approval from the Nagoya University Animal Experiment Committee (Protocol No. 26128, 27191, 28002, 29015) and conducted in accordance with the Regulations on Animal Experiments in Nagoya University. This study is reported in compliance with the ARRIVE guidelines (Animal Research: Reporting in Vivo Experiments), which included blinding and randomization among other quality control procedures to ensure reproducibility, transparency, and rigor of the experiments.

Isolation of human Muse and non-Muse cells

Human Muse cells and non-Muse cells were separated using fluorescence activated cell sorter (FACS) as green fluorescent protein (GFP)$^+$/SSEA-3$^+$ and GFP$^+$/SSEA-3$^-$ cell fractions, respectively, from human BM-MSCs (Lonza, PT-2501) labelled with GFP, as previously described.[22,23]

Perinatal HIE model and cell administration

The perinatal rat HIE model used seven-day-old Wistar/ST rat as previously described.[10] Briefly, rat pups were anesthetised with isoflurane. Then, the left common carotid arteries were double ligated and cut between the ligatures. After an hour recovery period, rats were subjected to 8% hypoxia at 37 °C in an incubator for 60 min. At 72 h after brain injury, animals received human Muse cells (1×10^4 cells), non-Muse cells (1×10^4 cells) in 0.1 mL saline, or vehicle (0.1 mL saline) via the right external jugular vein without immunosuppressive agents.

Tissue preparation

At 2, 4 weeks and 6 months after the treatment, rats were transcardially fixed with 4% paraformaldehyde and the brain was cut into paraffin or frozen sections.

Microglial activation assessments

To evaluate microglial activation, we co-cultured microglia cells (6-3 Microglia Cell Clone, COS-NMG-

6-3C, Cosmo Bio Co., Ltd., Tokyo, Japan) with Muse cells for 24 hours using transwell (Boyden chamber: FALCON Cell Culture Insert, Corning Life Sciences, Corning, NY, 353095). Then, we added lipopolysaccharide (LPS, serotype O55:B5, Sigma-Aldrich, St. Louis, MO) to the microglia cultures. Three or 24 hours after adding LPS, microglia cells were collected for quantitative polymerase chain reaction (qPCR).[24]

Quantitative polymerase chain reaction with the alu sequence specific primer

To assess the distribution of intravenously delivered human cells, we collected the brain, lung, liver and spleen at 2 and 4 weeks and processed them to qPCR with the Alu sequence specific primer (Alu PCR).[25]

Immunohistochemistry

We immunostained brain sections as previously described[25] with minor modifications, using primary antibodies either of anti-GFP (Abcam), anti-neuronal nuclei (NeuN; Millipore), anti-microtubule associated protein-2 (MAP-2; Sigma-Aldrich), anti-glutathione S-transferase pi (GST pi; MBL) or anti-glial fibrillary acidic protein (GFAP; Dako).

Brain image assessments

To assess brain metabolites, we performed ^{1}H-magnetic resonance spectroscopy (MRS) at 2 days after cell administration.[26] Additionally on day 2, positron emission tomography (PET) using [^{18}F] mitochondrial peripheral benzodiazepine receptor (PBR) ligands visualized the distribution of microglia activation.[27] To evaluate the cerebral blood flow (CBF), we conducted magnetic resonance imaging (MRI) -arterial spin labelling (ASL) at 2 days (acute phase) and 4 weeks (subacute phase) after administration. To assess the absolute brain tissue loss after hypoxic-ischemic (HI) insult, we employed MRI at 6 months after HIE.

Behavioral tests

At 4 weeks and 5 months after treatment, rats underwent 4 behavioral tests: the open-field,[28] novel object recognition,[29] active avoidance,[30] and cylinder tests,[31] in order to evaluate general locomotor activity and cognitive and motor functions.

Statistical analyses

Statistical analyses used the SPSS software version 26 (SPSS Inc., Chicago, IL, USA) and the JMP Pro 15 statistical software (SAS Institute, Cary, NC, USA). Shapiro-Wilk test was used to assess data distribution. Based on the results of the normality test, Student's t-test was used for two-group analyses about the engraftment in the peri-infarct area, and either one-way analysis of variance (ANOVA) followed by the Bonferroni post-hoc test or Kruskal-Wallis test followed by Steel-Dwass test was used to assess three or four groups for body weight gain, brain volume in MRI image, microglial activation, and behavioral tests. For the analysis of the data pertaining to MRS, PET, and MRI-ASL, a two-way ANOVA followed by the Bonferroni post-hoc test, with the two or three experimental groups and two regions (ipsilateral and contralateral sides of the brain) as the two independent variables, was used. For the analysis of the survival rate, we employed the Kaplan-Meier's method and log-rank test with Bonferroni correction. A P-value of less than 0.05 was considered statistically significant. All values correspond to the means with standard deviation.

Results

Characterization of human BM-Muse cells

We isolated SSEA-3$^+$ human-Muse and SSEA-3$^-$ human-non-Muse cells from human BM-MSCs by FACS (Supplemental Figure 1(a)). Single Muse cells formed embryoid body-like clusters in cultured suspension and displayed spontaneous differentiation into representative cell lineages of the three embryonic germ layers in gelatin-coated adherent culture, as described previously (Supplemental Figure 1(b) and (c)).[14,22]

Safety assessments

Analyses of survival rate at 6 months revealed no significant differences among the four groups: 85.0% (17/20) in the sham group, 76.7% (23/30) in the vehicle group, 75.0% (9/12) in the non-Muse-treated group and 81.8% (18/22) in the Muse cell-treated group (Figure 1(a)). The rats that received a HI insult, i.e. those in the vehicle, non-Muse and Muse cell-treated groups, showed lower weight gain over time, compared to the sham group. However, the body weight gain did not differ among the three HIE groups (Figure 1(b)). To confirm any signs of tumorigenicity in Muse cells, we performed macroscopic assessment of each organ and observed no detectable tumors in the any of the organs after Muse cell injection (Supplemental Figure 3).
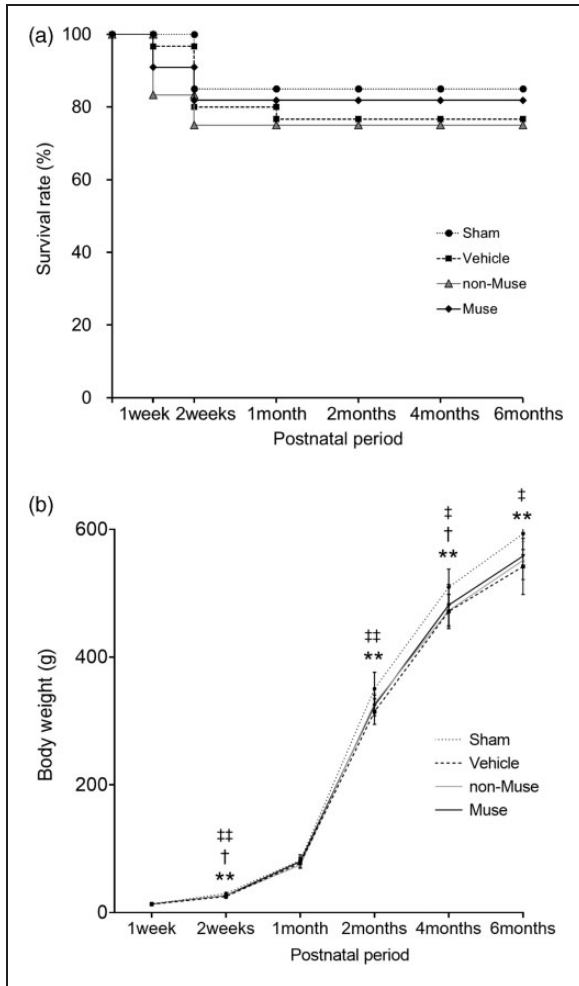
Figure 1. Survival rates and body weight measurements. (a) Time course of survival over 6 months, after birth (n = 20 for Sham, 30 for Vehicle, 12 for non-Muse and 22 for Muse cells). (b) Body weight gain over 6 months, after birth (n = 17 for Sham, 23 for Vehicle, 9 for non-Muse and 18 for Muse). Dotted line, Sham; dashed line, Vehicle; gray line, non-Muse, solid line, Muse. **p < 0.01, Sham vs. Vehicle; †p < 0.05, Sham vs. non-Muse; ‡p < 0.05 and ‡‡p < 0.01, Sham vs. Muse.

Muse cells reduce excess brain glutamate metabolites

MRS imaging in the vehicle group at 2 days after Muse cell administration demonstrated that the ipsilateral brain displayed significantly higher ratios of glutamate, glutamate+glutamine and lactate compared to the contralateral brain after HIE. Muse cell treatment significantly reduced these HIE-induced increments in the ipsilateral excitotoxic metabolites to 59.8%, 64.4%, and 26.4% of the vehicle group, respectively (Figure 2(a) and (b)).

Muse cells dampen microglial activation and normalize CBF

The standardized uptake value (SUV) of [18F]-PBR111 approximated microglial activity. At 2 days after Muse cell transplantation, [18F]-PBR111 PET imaging showed that the ipsilateral brain in the Muse cell-treated group exhibited significantly lower SUV than that the vehicle group (Figure 3(a) and (b)). In addition, *in vitro* experiment using the co-culture of microglia cells and Muse cells demonstrated that Muse cells suppressed the production of TNF-α at 3 hours and iNOS at 24 hours after LPS administration in microglial cells, suggesting the attenuation of microglial activation by Muse cells (Figure 3(c)). For MRI-ASL imaging, we focused on the CBF in the cortex and the thalamus. In both the acute 2 days and sub-acute 4 weeks phases, the ipsilateral side of the cortex displayed significantly reduced CBF in the vehicle and Muse cell-treated groups compared to the sham group. In the thalamus during the acute phase, the CBF across all groups did not differ in either ipsilateral or contralateral sides. However, in the sub-acute phase, the thalamus of contralateral hemisphere showed significantly lower CBF in the vehicle group than the sham group. The thalamus of the contralateral hemisphere in the Muse cell-treated group also exhibited a trend of lower CBF compared to the sham group but did not reach statistical significance. However, the Muse-cell-treated group displayed 22.3% and 10.2% higher CBF on the ipsilateral and contralateral hemispheres, respectively, compared to the vehicle group (Figure 4(a) and (b)).

Distribution of muse and non-Muse cells in HIE brain

At 2 weeks after treatment, Alu PCR detected human genomic DNA in the ipsilateral but not the contralateral hemisphere of Muse cell-treated rats. Both hemispheres of non-Muse cell-treated rats expressed no detectable human genomic DNA. In the lung, both Muse and non-Muse cell-treated rats expressed small amounts of human DNA (Figure 5(a)). At 4 weeks, human genomic DNA remained detectable only in the ipsilateral brain of the Muse cell-treated group, but not traceable neither in the contralateral brain, liver, spleen and lung, nor in any organ of the non-Muse cell-treated group (Figure 5(b)).

Neural markers expression in engrafted human-BM-Muse cells in the HIE brain

The brain volume did not differ among the three treated groups at 6 months after administration
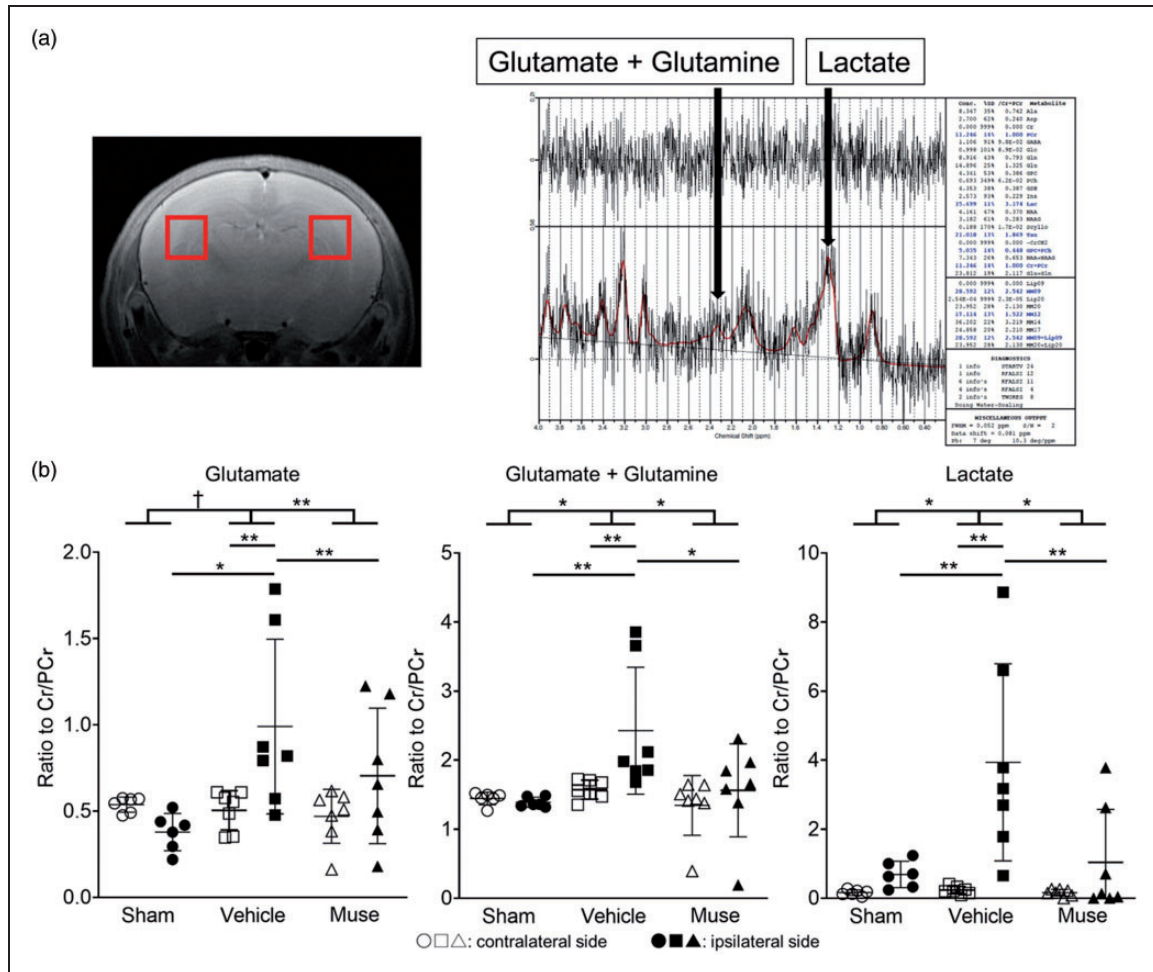
Figure 2. MRS imaging of the brain. (a) Representative MR images with ROI (left) and brain spectrum image (right) of the sham group. ROI is 2 mm-voxels in both cerebral hemispheres, including part of the cortex, hippocampus, white matter and thalamus. (b) Ratios of glutamate, glutamate+glutamine and lactate based on MRS imaging on day 2 (n = 6 for Sham, 7 for Vehicle, 7 for Muse). $^{†} = 0.050$, *$p < 0.05$ and **$p < 0.01$, Cr: Creatine, PCr: Phosphocreatine. White symbols correspond to contralateral side of brain and black ones represent ipsilateral side.

(Figure 6(a)). However, the Muse cell-treated group revealed GFP^{+} cells that expressed the neuronal marker, NeuN, at 2 days, 4 weeks and 6 months (Figure 6(b)). Moreover, in the peri-infarct area, Muse cells extensively distributed in the peri-infarct area, whereas non-Muse cells were scarcely detected (Figure 6(c), Supplemental Figure 2). At 6 months, 57.1% of GFP^{+} cells colocalized with the neuronal marker, MAP-2, and 21.1% GST-pi, an oligodendrocyte marker. None of the Muse cell-transplanted brains exhibited GFP^{+} cells that co-expressed the astrocytic marker GFAP as far as we observed (Figure 6(d)).

Muse cells attenuate HIE-induced behavioral impairments

The open-field test evaluated general locomotor activity, particularly hyperactivity. After 4 weeks, all four

groups registered no discernible differences in distance travelled. At 5 months post-treatment, the vehicle group significantly travelled longer than the sham group. The Muse cell-treated group travelled significantly shorter compared to the vehicle (p < 0.01) and non-Muse cell-treated groups (p < 0.05) (Figure 7(a)). Interestingly, the sham and Muse cell-treated groups did not significantly differ in distance travelled at 5 months. A novel object recognition test and an active avoidance test assessed cognitive functions.[29] In the novel object recognition test, the discrimination index (DI) in the Muse cell-treated group did not significantly differ from the sham group, whereas the DI in the vehicle group significantly decreased compared to the Muse cell-treated group at both 4 weeks and 5 months (p < 0.01). In contrast, the vehicle and non-Muse cell-treated groups did not differ at both time points, whereas the vehicle group showed significantly
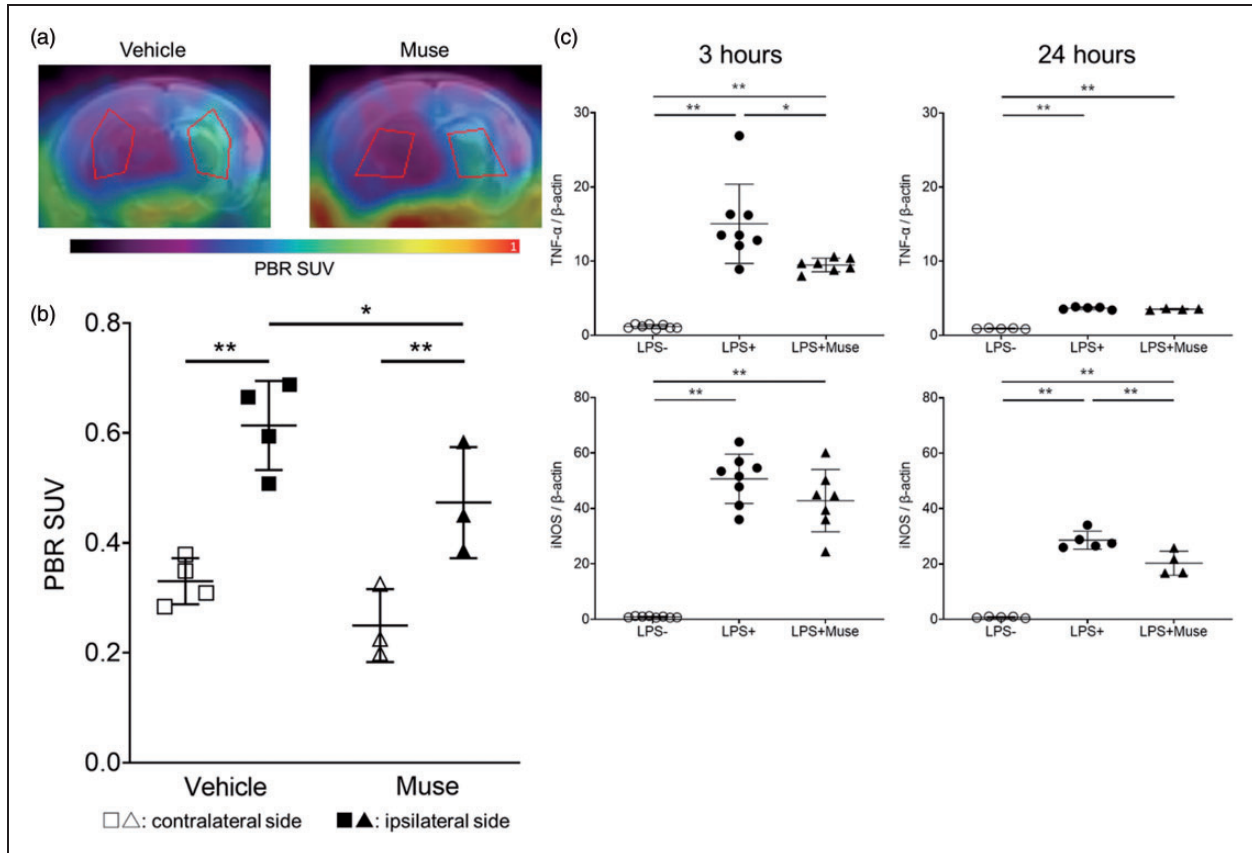
Figure 3. PET imaging of the brain and co-culture experiment of microglia cells. (a) Representative PET images overlaid with MRI images 2 days after cell administration in vehicle and Muse groups. ROIs correspond to the striatum and thalamus. (b) PBR SUV based on PET images at 2 days after cell administration (n = 4 for Vehicle, 3 for Muse). *p < 0.05 and **p < 0.01. White symbols represent contralateral side of brain and black correspond to the ipsilateral side. (c) *In vitro* experiment using the co-culture of microglia cells and Muse cells at 3 hours (left) and 24 hours (right) after LPS administration. White circle symbols (LPS-) correspond to microglia cells alone without LPS, black circle symbols (LPS+) represent microglia cells alone with LPS, and black triangle symbols (LPS+Muse) microglia co-cultured with Muse cells and LPS, respectively. (n = 8 for LPS-, 8 for LPS+, 7 for LPS+Muse at 3 hours, and n = 5 for LPS-, 5 for LPS+, 4 for LPS+Muse at 24 hours). *p < 0.05 and **p < 0.01.

lower DI compared to the sham group at 4 weeks and 5 months (p < 0.05) (Figure 7(b)). In the active avoidance test at 4 weeks, the avoidance rates in the vehicle-treated group on day 3 and day 4, and those in non-Muse-treated group on day 4 were statistically decreased compared with the avoidance rates of the sham group, whereas there was no significant difference in the avoidance rates between the Muse cell-treated and the sham group. In the active avoidance test at 5 months, the avoidance rates on day 3 and day 4 in the Muse cell-treated group significantly increased compared with those in the vehicle-treated group (p < 0.05). In contrast, the vehicle and non-Muse cell-treated groups did not differ (Figure 7(c)). Next, the cylinder test examined motor impairment.[30] Because our HIE model involved left cerebral injury, as expected, the vehicle group displayed significant preference for the left (ipsilateral) forepaw compared to

sham group at both 4 weeks and 5 months. In contrast, the Muse cell-treated group exhibited significantly reduced preference for the left forepaw than the vehicle-treated group both at 4 weeks (p < 0.05) and 5 months (p < 0.01), and the non-Muse cell-treated group at 5 months (p < 0.01) (Figure 7(d)). Importantly, the sham and Muse cell-treated groups did not differ at both 4 weeks and 5 months.

Discussion

In this study, intravenously administered human Muse cells, but not non-Muse cells (i.e., MSCs excluding Muse cells), exhibited long-term engraftment and expressed neuronal and glial cell markers in the HIE brain. MRS and PET showed that the human Muse cells attenuated the excessive levels of brain glutamate metabolites and dampened microglial
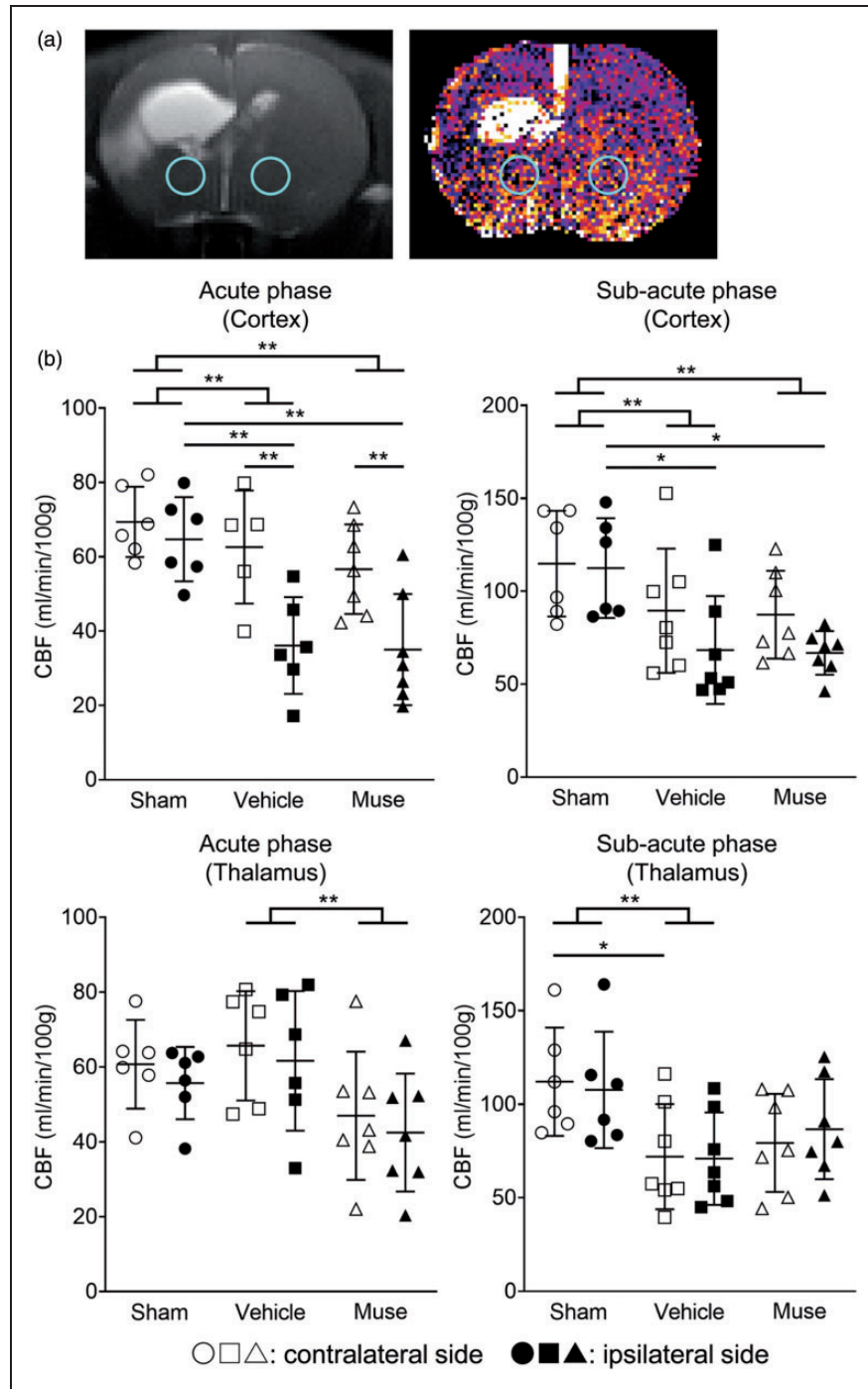
Figure 4. MRI-ASL imaging of the brain. (a) Representative MRI (left) and MRI-ASL (right) images at sub-acute phase after injection on the vehicle group. ROIs (blue circle) are set as 2 mm-voxels in the thalamus of each cerebral hemisphere. (b) CBF measurements in the cortex (upper) and thalamus (lower) based on MRI-ASL images at 2 days (acute phase, left) and 4 weeks (sub-acute phase, right) after cell administration (n = 6 for Sham, 7 for Vehicle, 7 for Muse). *p < 0.05 and **p < 0.01. White symbols represent contralateral side and black ones correspond to ipsilateral side.

activation in the acute phase of HIE. The Muse cell-treated animals displayed remarkable improvement in general locomotor activity, and cognitive and motor functions compared to the non-Muse cell- and vehicle-treated groups. These results collectively demonstrated robust and stable histological and behavioral benefits of human Muse cells in experimental HIE.
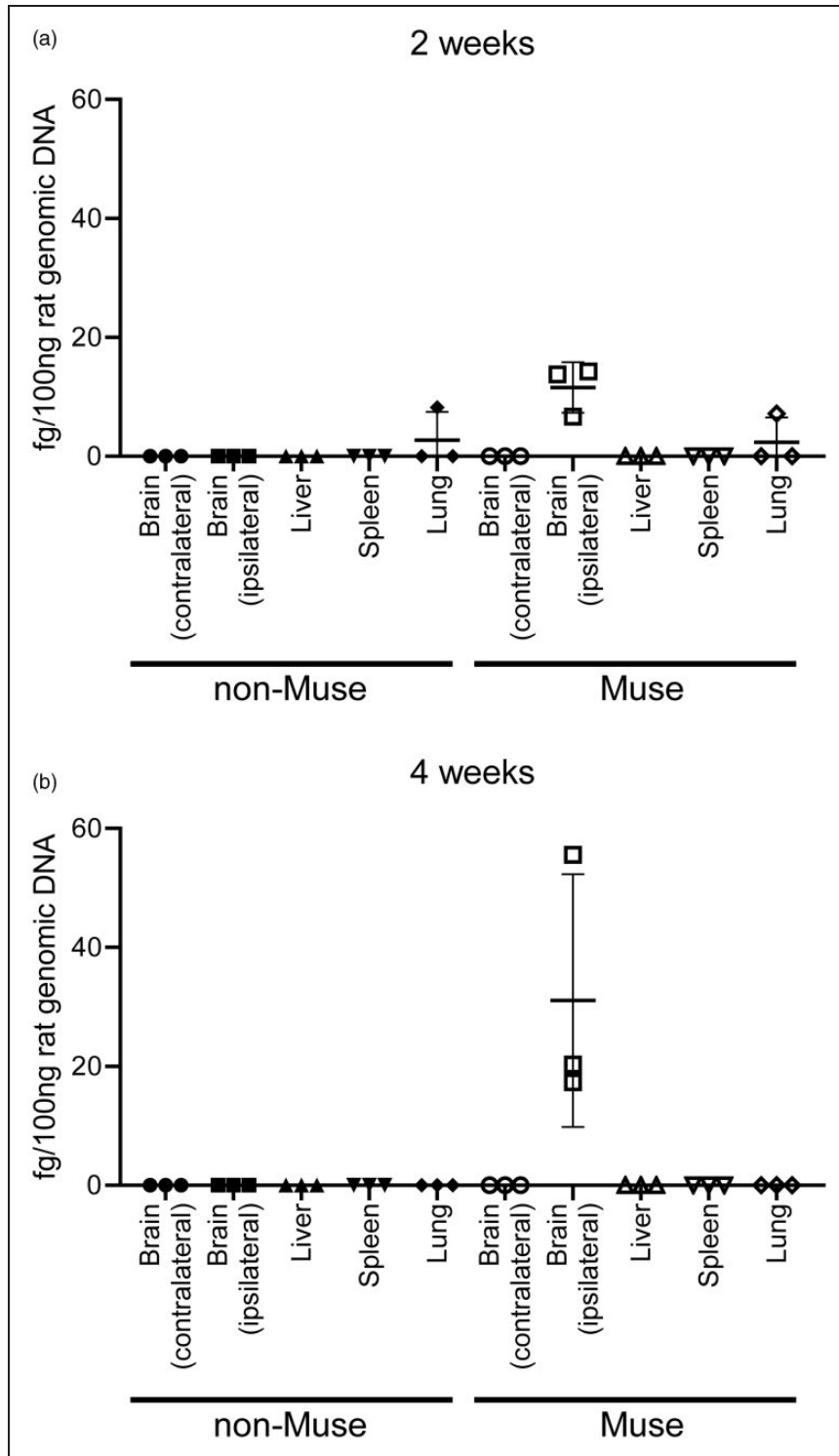
Figure 5. Detection of human Alu sequence by qPCR at 2 and 4 weeks after cell administration. (a) At 2 weeks, Muse cells were mainly detected at the ipsilateral brain and in the lung with lesser extent. Non-Muse cells were under detection limit in both the ipsilateral and contralateral brain (n = 3 for Muse, 3 for non-Muse). (b) At 4 weeks, Muse cells were still detectable in the ipsilateral brain and not in other organs, while non-Muse cells were under detection limit in the brain, liver, spleen and lung (n = 3 for Muse, 3 for non-Muse).
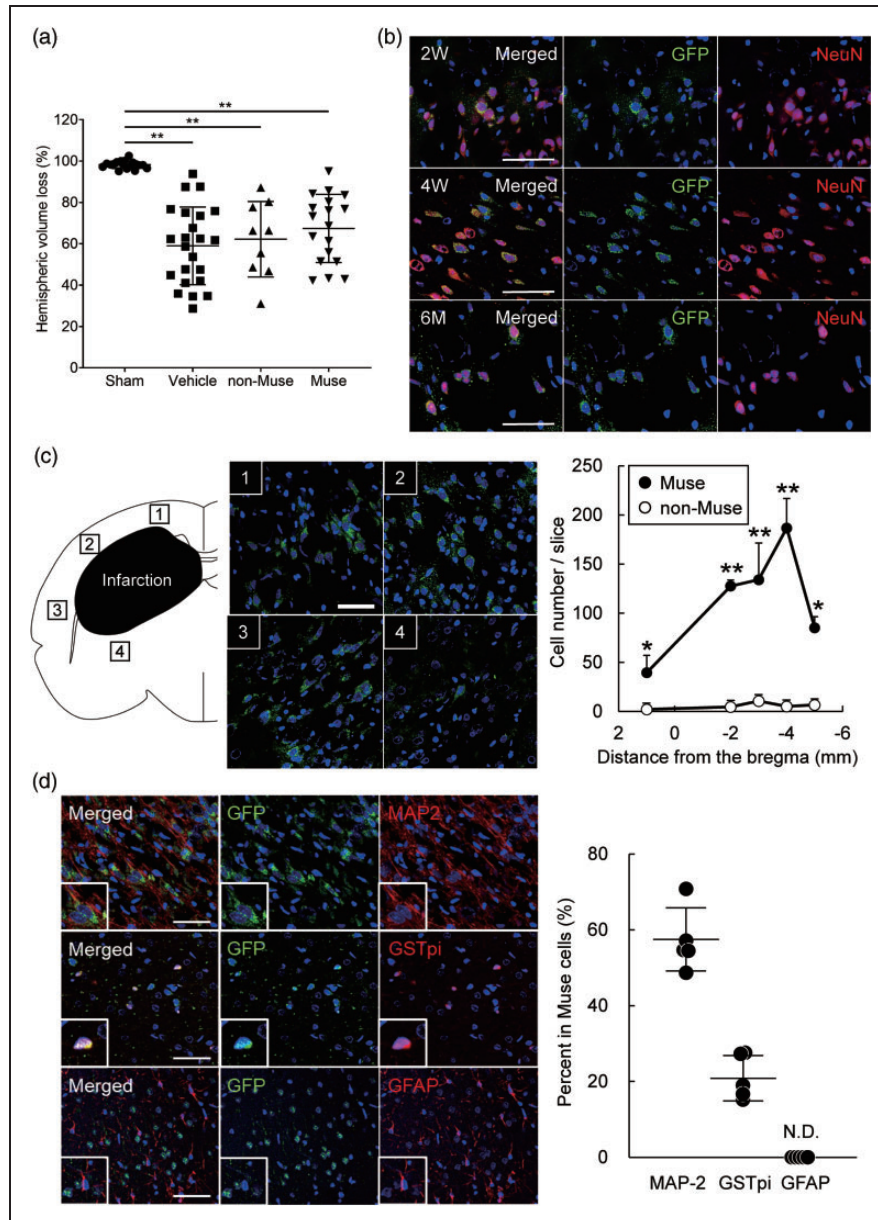
Figure 6. Engraftment of Muse cells in the brain after HIE. (a) Cerebral hemispheric volume loss at 6 months after HIE (n = 17 for Sham, 23 for Vehicle, 9 for non-Muse and 18 for Muse). (b) Differentiation of GFP$^+$ Muse cells after engraftment into HI-brain. Immunofluorescence for NeuN (red), GFP (green) and DAPI (blue) in the Muse cell-treated group brain at 2, 4 weeks and 6 months. Scale bars indicate 50 μm. (c) Immunofluorescence for GFP and DAPI in the Muse cell-treated group brain at 6 months after HIE. Scale bars indicate 50 μm. The number of GFP$^+$ cells per slice in the Muse and non-Muse-treated group brain at 6 months. *p < 0.05 and **p < 0.01. Black symbols represent Muse-treated group and white ones correspond to non-Muse-treated group. (d) Immunofluorescence for MAP-2 (upper, red), GST pi (middle, red), GFAP (lower, red) in GFP$^+$ (green) cells in the Muse cell-treated group brain at 6 months. Scale bars indicate 50 μm. The percentage of each marker within the total GFP$^+$ population in the Muse cell-treated group brain at 6 months. N.D., not detected.

A major finding of this study indicates that xenogeneic Muse cells survived and engrafted in the peri-infarct area of HIE brain as evidenced by neural marker-positive cells (NeuN, MAP-2 and GST pi) until 6 months post-transplantation without immuno-suppression. Such prolonged graft survival revealed no tumor formation in any of the transplanted groups. This observation concurred with previous reports demonstrating that Muse cells engraft and differentiate into neural cells following transplantation in a variety of injury models.[17,19,20,25] S1P- S1P receptor 2 axis plays an important role in the selective homing of
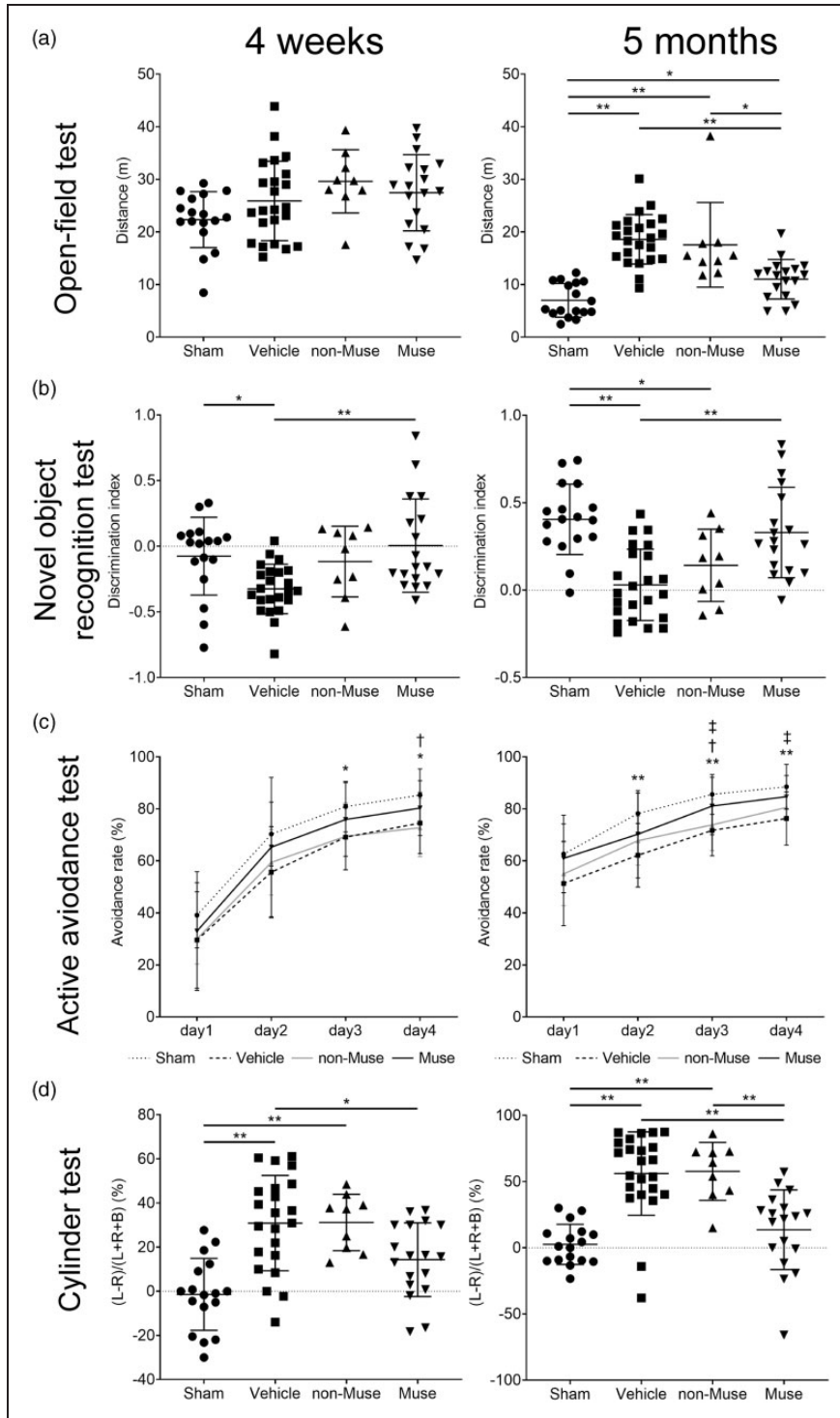
Figure 7. Behavioral tests at 4 weeks and 5 months after HIE. (a) Open-field test: the distance travelled at 4 weeks (left) and 5 months (right). *p < 0.05 and **p < 0.01. (b) Novel object recognition test: the discrimination index at 4 weeks (left) and 5 months (right). *p < 0.05 and **p < 0.01. (c) Active avoidance test: the change of avoidance rate at 4 weeks (left) and 5 months (right). Dotted line, Sham; dashed line, Vehicle; gray line, non-Muse; solid line, Muse. *p < 0.05 and **p < 0.01, Sham vs. Vehicle; †p < 0.05, Sham vs. non-Muse; ‡p < 0.05, Muse vs. Vehicle. (d) Cylinder test: the preference for left (ipsilateral) forepaw calculated at 4 weeks (left) and 5 months (right). *p < 0.05 and **p < 0.01; n = 17 for Sham, 23 for Vehicle, 9 for non-Muse and 18 for Muse, for (a), (b), (c) and (d).

intravenously administered Muse cells to damaged site.[17] That peripherally delivered Muse cells migrated and survived efficiently in the HIE brain addresses the crucial translational issue of low graft survival routinely seen with many stem and progenitors cells transplanted in experimental CNS disorders.[32,33] The damaged brain harbors inflammatory cytokines, nitric oxide synthase (NOS) and free radical products, thus creating a hostile environment detrimental for survival of transplanted cells.[34–36] However, Muse cells pose as stress tolerant cells, allowing them to easily adapt to such harsh environment mounted by brain insults like HIE.[37] Muse cells secrete prosurvival factors such as 14-3-3 proteins and serpins, which play important roles in regulating the cellular response to DNA damage.[38] Additionally in Muse cells, increased non-homologous end joining enzyme activity following injury results in efficient activation of the DNA damage repair system within 6 hours.[39] In addition, the timing of cell administration may affect survival and neuronal differentiation. Sato et al. reported that during the acute phase of brain injury, early transplantation of neural stem cells at 24 hours after insult led to reduced number of the surviving cells and higher rates of astroglial differentiation, whereas in later transplantation, after the peak of inflammation, astroglial differentiation decreased, and survival and neural differentiation restored to the same extent as in the unaffected brain.[40] In the present study, Muse cells were administered at 72 h after brain injury, which might be a more favorable timing for Muse cells to survive and differentiate into neurons and oligodendrocytes. Furthermore, "spontaneous differentiation into tissue-compatible cells after homing" is one of the unique characteristics of Muse cells. Indeed, previous reports demonstrated spontaneous differentiation of engrafted Muse cells into tissue constituent cells in a variety of injury models such as stroke, liver damage, acute myocardial infarction and chronic kidney disease.[17,19,20,25] Direct cell-cell interaction between Muse cells and the injured host cells might be essential for the differentiation of Muse cells although additional studies are warranted to reveal the precise mechanism.[20]

In concert with replacement of dead or dying cells, Muse cells exert trophic effects critically relevant to neural repair.[21] Although MRI revealed that Muse and non-Muse cells did not reduce HIE-induced brain volume loss compared to the vehicle group at 6 months, MRS showed that Muse cells substantially suppressed the upregulation of lactate and glutamate+-glutamine in the ipsilateral brain. Increased lactate and excess glutamate accompany hypoxia (oxygen-deficient state), which in turn activates NOS and the release of free radicals, altogether triggering irreversible neuronal cell injury.[41,42] Muse cells may suppress cell death by activating DNA damage repair system and secreting essential factors that regulate ox-redox activities.[38,39] Here, the transplanted Muse cells possibly blocked the HIE-induced anaerobic metabolism, thereby arresting the downstream neuronal cell injury.

Similarly, our PET results revealed that Muse cells effectively abrogated microglial activation. In addition, in the in vitro co-culture experiment of microglial cells and Muse cells, Muse cells suppressed the mRNA expression of TNF-α and iNOS, which are important factors of microglial activity (Figure 3(c)).[43,44] Activated microglia closely approximate the onset and progression of the key secondary cell death process of neuroinflammation.[45] Targeting microglial activation, which features prominently in the pathological cascade of adult stroke and perinatal HIE, stands as an attractive reparative mechanism of Muse cells.

Meaningful functional improvements in motor and cognitive functions over a long period of 5 months represent vital efficacy readouts for translating Muse cells to the clinic. Preliminary data using dynamic plantar test also showed that Muse cells ameliorated sensory impairment induced by HIE (Supplemental Figure 4). That HIE entails an amalgam of behavioral abnormalities, demonstrating that Muse cells promoted functional recovery of motor, cognitive, and sensorimotor functions provide a stringent platform for evaluating its potential clinical efficacy. Equally an important translational guidance pertains to the enhanced behavioral improvement at 5 months post-transplantation, suggesting long-term stable effects even with a single intravenous injection of Muse cells. This sustained functional recovery may be mediated by the robust engraftment and neural differentiation of Muse cells.

Safety outcomes serve as another crucial guiding criterion for clinical translation of Muse cells. Pulmonary embolism and increased mortality have been documented with intravenous administration of cells.[10] In the present study, however, Muse cells neither promoted overt lung embolism nor worsened mortality. Examination of transplanted Muse cells revealed no detectable tumors up to the 6-month study period (Supplemental Figure 3), supporting previous reports of low risk of tumorigenicity of Muse cells even when transplanted in immunodeficient animals, thus resembling the solid safety profile of MSCs.[22,25,46] Moreover, in the present study, the cell dose of Muse cells was 1×10^4 cells, which was less than one-tenth compared to the previous reports of MSCs.[47] Moreover, when contemplating the practical caveats of clinical transplantation, it is likely that the higher the number of cells to be administered will lead to higher risk and cost of such transplant regimen. Since MSCs contain only a few percent of Muse cells and Muse cells exert more therapeutic effect than non-Muse cells,

transplanting Muse cells alone rather than the whole MSCs will de-risk and lower the cost of an effective cell therapy. Currently, several clinical trials have been conducted by intravenous drip of donor-derived allogeneic Muse cells without HLA matching and immunosuppressant treatment. For neonates, the infusion of a small number of Muse cells similarly represents a low risk and highly efficacious transplant approach.

In conclusion, intravenous administration of Muse cells dramatically ameliorated the behavioral abnormalities in the perinatal HIE model possibly through engraftment of Muse cells in the injured brain and their differentiation into neural cells, coupled with suppression of excitotoxic brain glutamate metabolites and attenuation of microglial activation. The present study supports the feasibility of intravenously administered donor-derived allogeneic Muse cells for ongoing clinical trials in CNS disorders without HLA-matching and long-term immunosuppressant,[48] which may be extended to HIE.

Declaration of conflicting interests

The author(s) declared the following potential conflicts of interest with respect to the research, authorship, and/or publication of this article: YS and SSh have a collaborative research and developmental agreement for perinatal disease with Life Science Institute Inc.(LSII). SSh is making a collaborative research and developmental agreement for the other disease, and has a contract for consulting with LSII. YS, TS, SSh, MM, MH and MD have a patent for the application of Muse cells for treatment of perinatal brain damage and the other indication. SW, YK and MD are parties to a co-development agreement with LSII. MD have a patent for the application of Muse cells for treatment of cerebral infarction. SW and MD have a patent for Muse cells, and the isolation method thereof licensed to LSII.

Authors' contributions

TS, KU, YK, MT, SW and MD were directly involved in animal experiments. MT, TT, SSa, and HI were involved in experiments with MRS, PET and MRI-ASL. YK, SW and MD prepared the cells and evaluated the fate of administrated cells. TS, YS, SSh, MT, KI, YI, MM, HH, YT, CVB and MH conceptualised and designed the study. TS, YS, KU, MM and CVB interpreted the data. TS draughted the initial manuscript, and YS, MT, HH, YT, MD, CVB and MH critically reviewed the manuscript. All authors approved the final manuscript and are accountable for all the work.

Data and materials availability

The datasets and materials generated during the current study are available from the corresponding author upon reasonable request.

ORCID iDs

Toshihiko Suzuki (iD) https://orcid.org/0000-0001-8760-1404
Masahiro Tsuji (iD) https://orcid.org/0000-0002-1540-3641
Shinobu Shimizu (iD) https://orcid.org/0000-0001-9066-3489
Hideki Hida (iD) https://orcid.org/0000-0002-9679-4508
Cesar V Borlongan (iD) https://orcid.org/0000-0002-2966-9782

Supplemental material

Supplemental material for this article is available online.

References

1. Hayakawa M, Ito Y, Saito S, et al. Incidence and prediction of outcome in hypoxic-ischemic encephalopathy in Japan. *Pediatr Int* 2014; 56: 215–221.
2. Volpe JJ. Neonatal encephalopathy: an inadequate term for hypoxic-ischemic encephalopathy. *Ann Neurol* 2012; 72: 156–166.
3. Lyden PD, Lamb J, Kothari S, et al. Differential effects of hypothermia on neurovascular unit determine protective or toxic results: toward optimized therapeutic hypothermia. *J Cereb Blood Flow Metab* 2019; 39: 1693–1709.
4. Shankaran S, Laptook AR, Ehrenkranz RA, et al.; National Institute of Child Health and Human Development Neonatal Research Network. Whole-body hypothermia for neonates with hypoxic-ischemic encephalopathy. *N Engl J Med* 2005; 353: 1574–1584.
5. Borlongan CV, Nguyen H, Lippert T, et al. May the force be with you: transfer of healthy mitochondria from stem cells to stroke cells. *J Cereb Blood Flow Metab* 2019; 39: 367–370.
6. Sato Y, Nakanishi K, Hayakawa M, et al. Reduction of brain injury in neonatal hypoxic-ischemic rats by intracerebroventricular injection of neural stem/progenitor cells together with chondroitinase ABC. *Reprod Sci* 2008; 15: 613–620.
7. Sato Y and Oohira A. Chondroitin sulfate, a major niche substance of neural stem cells, and cell transplantation therapy of neurodegeneration combined with niche modification. *Curr Stem Cell Res Ther* 2009; 4: 200–209.
8. Hattori T, Sato Y, Kondo T, et al. Administration of umbilical cord blood cells transiently decreased hypoxic-ischemic brain injury in neonatal rats. *Dev Neurosci* 2015; 37: 95–104.
9. Nakanishi K, Sato Y, Mizutani Y, et al. Rat umbilical cord blood cells attenuate hypoxic-ischemic brain injury in neonatal rats. *Sci Rep* 2017; 7: 44111.

10. Sugiyama Y, Sato Y, Kitase Y, et al. Intravenous administration of bone marrow-derived mesenchymal stem cell, but not adipose tissue-derived stem cell, ameliorated the neonatal hypoxic-ischemic brain injury by changing cerebral inflammatory state in rat. *Front Neurol* 2018; 9: 757–709.

11. Fu Y, Karbaat L, Wu L, et al. Trophic effects of mesenchymal stem cells in tissue regeneration. *Tissue Eng Part B Rev* 2017; 23: 515–528.

12. Xin H, Liu Z, Buller B, et al. MiR-17-92 enriched exosomes derived from multipotent mesenchymal stromal cells enhance axon-myelin remodeling and motor electrophysiological recovery after stroke. *J Cereb Blood Flow Metab*. Epub ahead of print 18 August 2020. DOI: 10.1177/0271678X20950489.

13. Trounson A and McDonald C. Stem cell therapies in clinical trials: progress and challenges. *Cell Stem Cell* 2015; 17: 11–22.

14. Wakao S, Kitada M, Kuroda Y, et al. Multilineage-differentiating stress-enduring (muse) cells are a primary source of induced pluripotent stem cells in human fibroblasts. *Proc Natl Acad Sci U S A* 2011; 108: 9875–9880.

15. Wakao S, Kuroda Y, Ogura F, et al. Regenerative effects of mesenchymal stem cells: contribution of muse cells, a novel pluripotent stem cell type that resides in mesenchymal cells. *Cells* 2012; 1: 1045–1060.

16. Dezawa M. Muse cells provide the pluripotency of mesenchymal stem cells: direct contribution of muse cells to tissue regeneration. *Cell Transplant* 2016; 25: 849–861.

17. Yamada Y, Wakao S, Kushida Y, et al. S1P-S1PR2 axis mediates homing of muse cells into damaged heart for Long-Lasting tissue repair and functional recovery after acute myocardial infarction. *Circ Res* 2018; 122: 1069–1083.

18. Kushida Y, Wakao S and Dezawa M. Muse cells are endogenous reparative stem cells. *Adv Exp Med Biol* 2018; 1103: 43–68.

19. Uchida N, Kushida Y, Kitada M, et al. Beneficial effects of systemically administered human muse cells in adriamycin nephropathy. *J Am Soc Nephrol* 2017; 28: 2946–2960.

20. Iseki M, Kushida Y, Wakao S, et al. Muse cells, non-tumorigenic pluripotent-like stem cells, have liver regeneration capacity through specific homing and cell replacement in a mouse model of liver fibrosis. *Cell Transplant* 2017; 26: 821–840.

21. Kinoshita K, Kuno S, Ishimine H, et al. Therapeutic potential of adipose-derived SSEA-3-positive muse cells for treating diabetic skin ulcers. *Stem Cells Transl Med* 2015; 44: 146–155.

22. Kuroda Y, Kitada M, Wakao S, et al. Unique multipotent cells in adult human mesenchymal cell populations. *Proc Natl Acad Sci U S A* 2010; 107: 8639–8643.

23. Kuroda Y, Wakao S, Kitada M, et al. Isolation, culture and evaluation of multilineage-differentiating stress-enduring (muse) cells. *Nat Protoc* 2013; 8: 1391–1415.

24. Imai K, Kotani T, Tsuda H, et al. Neuroprotective potential of molecular hydrogen against perinatal brain injury via suppression of activated microglia. *Free Radic Biol Med* 2016; 91: 154–163.

25. Uchida H, Niizuma K, Kushida Y, et al. Human muse cells reconstruct neuronal circuitry in subacute lacunar stroke model. *Stroke* 2017; 48: 428–435.

26. Saito S, Takahashi Y, Ohki A, et al. Early detection of elevated lactate levels in a mitochondrial disease model using chemical exchange saturation transfer (CEST) and magnetic resonance spectroscopy (MRS) at 7T-MRI. *Radiol Phys Technol* 2019; 12: 46–54.

27. Guo Q, Colasanti A, Owen DR, et al. Quantification of the specific translocator protein signal of 18F-PBR111 in healthy humans: a genetic polymorphism effect on in vivo binding. *J Nucl Med* 2013; 54: 1915–1923. DOI:10.2967/jnumed.113.121020.

28. Han S, Tai C, Westenbroek RE, et al. Autistic-like behaviour in Scn1a+/– mice and rescue by enhanced GABA-mediated neurotransmission. *Nature* 2012; 489: 385–390.

29. Antunes M and Biala G. The novel object recognition memory: neurobiology, test procedure, and its modifications. *Cogn Process* 2012; 13: 93–110.

30. Ichinohashi Y, Sato Y, Saito A, et al. Dexamethasone administration to the neonatal rat results in neurological dysfunction at the juvenile stage even at low doses. *Early Hum Dev* 2013; 89: 283–288.

31. Schallert T, Fleming SM, Leasure JL, et al. CNS plasticity and assessment of forelimb sensorimotor outcome in unilateral rat models of stroke, cortical ablation, parkinsonism and spinal cord injury. *Neuropharmacology* 2000; 39: 777–787.

32. Yabuki H, Wakao S, Kushida Y, et al. Human multilineage-differentiating stress-enduring cells exert pleiotropic effects to ameliorate acute lung ischemia-reperfusion injury in a rat model. *Cell Transplant* 2018; 27: 979–993.

33. Hadley G, Beard DJ, Couch Y, et al. Rapamycin in ischemic stroke: old drug, new tricks? *J Cereb Blood Flow Metab* 2019; 39: 20–35.

34. Yamauchi T, Kuroda Y, Morita T, et al. Therapeutic effects of human multilineage-differentiating stress enduring (MUSE) cell transplantation into infarct brain of mice. *PLoS One* 2015; 10: e0116009.

35. Johnston MV, Trescher WH, Ishida A, et al. Novel treatments after experimental brain injury. *Semin Neonatol* 2000; 5: 75–86.

36. Tseng N, Lambie SC, Huynh CQ, et al. Mitochondrial transfer from mesenchymal stem cells improves neuronal metabolism after oxidant injury in vitro: the role of Miro1. *J Cereb Blood Flow Metab*. Epub ahead of print 5 June 2020. DOI: 10.1177/0271678X20928147.

37. Heneidi S, Simerman AA, Keller E, et al. Awakened by cellular stress: isolation and characterization of a novel population of pluripotent stem cells derived from human adipose tissue. *PLoS One* 2013; 8: e64752.

38. Alessio N, Ozcan S, Tatsumi K, et al. The secretome of MUSE cells contains factors that may play a role in regulation of stemness, apoptosis and immunomodulation. *Cell Cycle* 2017; 16: 33–44.

39. Alessio N, Squillaro T, Ozcan S, et al. Stress and stem cells: adult muse cells tolerate extensive genotoxic stimuli

better than mesenchymal stromal cells. *Oncotarget* 2018; 9: 19328–19341.

40. Sato Y, Shinjyo N, Sato M, et al. Grafting of neural stem and progenitor cells to the hippocampus of young, irradiated mice causes gliosis and disrupts the granule cell layer. *Cell Death Dis* 2013; 4: e591.

41. Tan WK, Williams CE, During MJ, et al. Accumulation of cytotoxins during the development of seizures and edema after hypoxic-ischemic injury in late gestation fetal sheep. *Pediatr Res* 1996; 39: 791–797.

42. McCaig C, Ataliotis P, Shtaya A, et al. Induction of the cell survival kinase Sgk1: a possible novel mechanism for α-phenyl-N-tert-butyl nitrone in experimental stroke. *J Cereb Blood Flow Metab* 2019; 39: 1111–1121.

43. Yu Z, Fukushima H, Ono C, et al. Microglial production of TNF-alpha is a key element of sustained fear memory. *Brain Behav Immun* 2017; 59: 313–321.

44. Marques CP, Cheeran MC, Palmquist JM, et al. Microglia are the major cellular source of inducible nitric oxide synthase during experimental herpes encephalitis. *J Neurovirol* 2008; 14: 229–238.

45. Taylor RA and Sansing LH. Microglial responses after ischemic stroke and intracerebral hemorrhage. *Clin Dev Immunol* 2013; 2013: 746068–746011.

46. Ogura F, Wakao S, Kuroda Y, et al. Human adipose tissue possesses a unique population of pluripotent stem cells with nontumorigenic and low telomerase activities: potential implications in regenerative medicine. *Stem Cells Dev* 2014; 23: 717–728.

47. Archambault J, Moreira A, McDaniel D, et al. Therapeutic potential of mesenchymal stromal cells for hypoxic ischemic encephalopathy: a systematic review and meta-analysis of preclinical studies. *PLoS One* 2017; 12: e0189895.

48. Abe T, Aburakawa D, Niizuma K, et al. Intravenously transplanted human multilineage-differentiating stress-enduring cells afford brain repair in a mouse lacunar stroke model. *Stroke* 2020; 51: 601–611.